Supplementary information

Sampling Techniques

Etang de la Gruère (EGR) in the Jura Mountains, Switzerland, is a raised ombrotrophic bog consisting in up to 650 cm of peat directly overlying lacustrine clay. Two cores representing the entire Holocene and extending into the Late Glacial were collected and analyzed for major and trace elements including REE, neodymium isotopes (expressed as εNd values) and pollen. Ages were obtained using ^{210}Pb analysis and ^{14}C for respectively the uppermost and deeper layers, and allow the construction of two robust age-depth models. The low-resolution cores (EGR 2P+2K) was sliced every 3 cm for the upper meter and every 10 cm for the underlying 5.5 m. The subsamples were used to reconstruct the atmospheric Pb deposition since the Late Glacial, ca. 14,500 cal. yr B.P. (Shotyk et al., 2001). All subsamples were re-analysed for REE using Q-ICP-MS, and selected subsamples were measured for Nd isotopes using MC-ICP-MS. The high-resolution cores were cut every 1 cm (EGR 2G) and 2 cm (EGR 2A), respectively and analyzed for Ti (Roos-Barraclough et al., 2002) and pollen (Roos-Barraclough et al., 2004). Based on the Ti concentrations, selected samples from these cores were measured for REE and Nd isotopes using Q-ICP-MS and MC-ICP-MS, respectively. One centimeter in the lowest decomposed part (catotelm) at EGR represents ~30 years of peat accumulation, meaning that the high-resolution core (2A) has a 60-year resolution while the low-resolution core (2P) had only a 300-yr resolution.

In this manuscript, diagrams are built on combined data of the low-resolution and high-resolution cores.

Analytical. Geochemistry

Trace elements were measured in peat after preparation following Givelet et al.(2004). Peat powders for the entire cores were measured for major and some trace elements by home-made XRF devices (Cheburkin and Shotyk, 2005, 1996) at IES, Heidelberg. They were also digested using a HNO_3-HBF_4 mixture in a high-pressure microwave (Krachler et al., 2002a,b) and measured using Q-ICP-MS at Strasbourg and Jülich (Krachler et al., 2003). Digested solutions were also used for Nd analyses after Nd purification using classical. REE and Nd extraction scheme (Pin and Zalduegui, 1997) and then were measured using a Nu plasma MC-ICPMS at DSTE, Brussels.

Age-depth Models for the Two Cores

Radiocarbon preparation, measurements and age dating of the two cores are detailed in Shotyk et al (2001) and Roos-Barraclough et al (2004). We have established the best age-depth model using a fifth polynomial relationship (Fig. DR1) for both records. Compared to linear interpolation (Fig. DR2), it avoids large shifts in modelled peat accumulation. However other models like the one obtained using Oxcal (Bronk Ramsey, C., 2001) give similar

chronologies, especially for the events of interest (see Fig. 2 of the main text, and Table DR1). We use also the Bayesian approach to model the age-depth relationship of the 2 cores using "Bacon" (Blaauw and Christen, 2011). It also gives similar information (Figs. DR3-DR4), even if the high resolution core allows to evidence some peaks (i.e. the Younger Dryas double peaks), and to better discriminate several events. Fig. DR5 shows also that there is no high difference between the dust deposition chronology as calculated by the 5th polynomial relationship and "Bacon".

Validation of the Peat Core as Archive of Dust Deposition: Ti Concentrations in Both Cores

The Ti records are similar in both cores (Fig. DR.5), confirming the reproducibility of the atmospheric record at EGR. As already noticed by Shotyk et al. (2001), Ti concentrations are enhanced around 12 cal. kyr B.P., *i.e.* around the Younger Dryas (YD). Between 10 and 8 kyr ago, the high-resolution core (<50y/sample) records two events, related respectively to (1) the Vasset-Killian (VK) eruption in French Massif Central, (2) a larger dust flux around 8.4 cal. kyr B.P., called Early-Middle Holocene Transition (EMHT). These two events were already suggested yet undistinguished by a unique peak recorded in the low-resolution core (Roos. The Nd isotope signature similar for this peak and for the VKT peak of the high-resolution core means that the EMHT peak was not visible in the low-resolution core. A third event also occurred around 7.5 cal. kyr B.P., which is not visible in the low-resolution core. Ti concentrations increase in both cores after ~6 cal. kyr B.P. until ~3 cal. kyr B.P., when a stabilisation of the dust supply occurred.

Pollen Diagram (Fig. DR6***)***

The preparation of pollen samples included the use of HCl, KOH and HF, and acetolysis. Pollen samples are mounted in glycerine. All pollen analysis was carried out at the Geobotanical Institute, Bern. Data are available from the European Pollen Database (http://www.europeanpollendatabase.net).

Calculation of Dust Deposition in Rate at EGR

Dust deposition rate (g m^{-2} y^{-1}) was calculated as follow:
Dust Deposition Rate = 10 x $[Ti]_{peat}$ x Density /t x 1/$[Ti]_{UCC}$ /1000

Where $[Ti]_{peat}$ is the Ti concentration (mg kg^{-1}) in core EGR2A+2F, Density the bulk dry peat density (g cm^{-3}) , t the time interval (years), $[Ti]_{UCC}$ the Ti concentration (mg kg^{-1}) in the Upper Continental Crust (Mc Lennan, 2001) taken here as representative of average dust deposited on the bog.

Additional References

Blaauw, M., and Christen, J.A., 2011, Flexible Paleoclimate Age-Depth Models Using an Autoregressive Gamma Process: Bayesian Analysis, v.6, p.457-474

Bronk Ramsey, C., 2001, Development of the Radiocarbon calibration program OxCal: Radiocarbon, v.43, p.355-363.

Cheburkin, A.K. and Shotyk, W., 1996, An Energy-dispersive Miniprobe Multielement Analyser (EMMA) for direct analysis of Pb and other trace elements in peats: Fresenius Journal of Analytical. Chemistry, v.354, p.688-691.

Cheburkin, A. and Shotyk, W., 2005, An energy-dispersive XRF spectrometer for Ti analysis (TITAN): X-Ray Spectrometry, v.34, p.69-72.

Givelet, N., Le Roux, G., Cheburkin, A., Chen, B., Frank, J., Goodsite, M., Kempter, H., . Krachler, M., Noernberg, T., Rausch, N., Rheinberger, S., Roos-Barraclough, F., Sapkota, A., Scholz, C., Shotyk, W., 2004, Suggested protocol for collecting, handling and preparing peat cores and peat samples for physical, chemical, mineralogical and isotopic analyses: Journal of Environmental Monitoring, v.6(5), p.481–492

Krachler, M., Mohl, C., Emons, H. and Shotyk, W., 2002a: Analytical. procedures for the determination of selected trace elements in peat and plant samples by inductively coupled plasma spectrometry: Spectrochimica Acta Part B, v.57, p.1277-1289

Krachler, M., Mohl, C., Emons, H. and Shotyk, W., 2002b: Influence of digestion procedures on the determination of rare earth elements in peat and plant samples by USN-ICP-MS: Journal of Analytical.Atomic Spectrometry, v.17, p.844-851.

Krachler, M., Mohl, C., Emons, H. and Shotyk, W., 2003, Two thousand years of atmospheric rare earth element (REE) deposition as revealed by an ombrotrophic peat bog profile, Jura Mountains, Switzerland: Journal of Environmental Monitoring, v.5, p.111-121.

McLennan, S.M., 2001, Relationships between the trace element composition of sedimentary rocks and upper continental crust: G-cubed, v.2, 2000GC000109, online

Pin, C. and Zalduegui, J.S., 1997, Sequential separation of light rare-earth elements, thorium and uranium by miniaturized extraction chromatography: Application to isotopic analyses of silicate rocks: Analytica Chimica Acta, v. 339(1-2), p.79-89.

Roos-Barraclough, F., van der Knaap, W.O., van Leeuwen, J.F.N. and Shotyk, W., 2004, A Late-glacial and Holocene record of climatic change from a Swiss peat humification profile: Holocene, v.14(1), p.7-19.

Shotyk, W. , Weiss D., Kramers J.D., Frei R., Cheburkin A.K., Gloor M.and Reese, S., 2001, Geochemistry of the peat bog at Etang de la Gruère, Jura Mountains, Switzerland, and its record of atmospheric Pb and lithogenic trace metals (Sc, Ti, Y, Zr, and REE) since 12,370 14C B.P.: Geochimica et Cosmochimica Acta, v.65(14), p. 2337-2360.

Table DR 1. Values of dust flux and age estimates of major dust peaks at Etang de la Gruère as given by 5th polynomial fit, Oxcal (P-sequence) and Bacon age-depth models.

Dust peaks	Depth (EGR 2A)	Dust flux ($g\ m^{-2}\ y^{-1}$)	5th polynomial estimate	Oxcal Interval estimate	Bacon histogram (Y-axis: frequency in %)
YD2	554 cm	8.6	12200±310	12750-12190	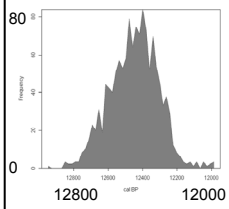
YD1	544 cm	12.8	11860±300	12260-11430	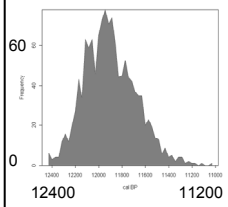
VKT2	436 cm	8.9	9060±180	9280-9010	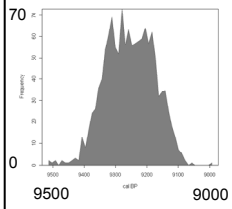
VKT1	430 cm	5.8	8980±175	9210-8930	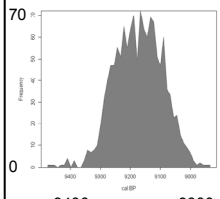

Dust peaks	Depth (EGR 2A)	Dust flux (g m^{-2} y^{-1})	5th polynomial estimate	Oxcal Interval estimate	Bacon histogram (Y-axis: frequency in %)
EMHT1	**380 cm**	**5.7**	**8440±140**	**8530-8390**	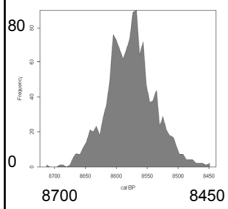
EMHT	**376 cm**	**14**	**8400±140**	**8480-8310**	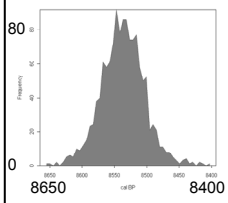
7.2	**296 cm**	**5.2**	**7440±140**	**7290-7000**	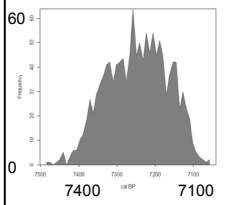
6	**234 cm**	**2.5**	**5960±160**	**6530-6270**	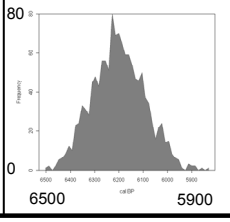

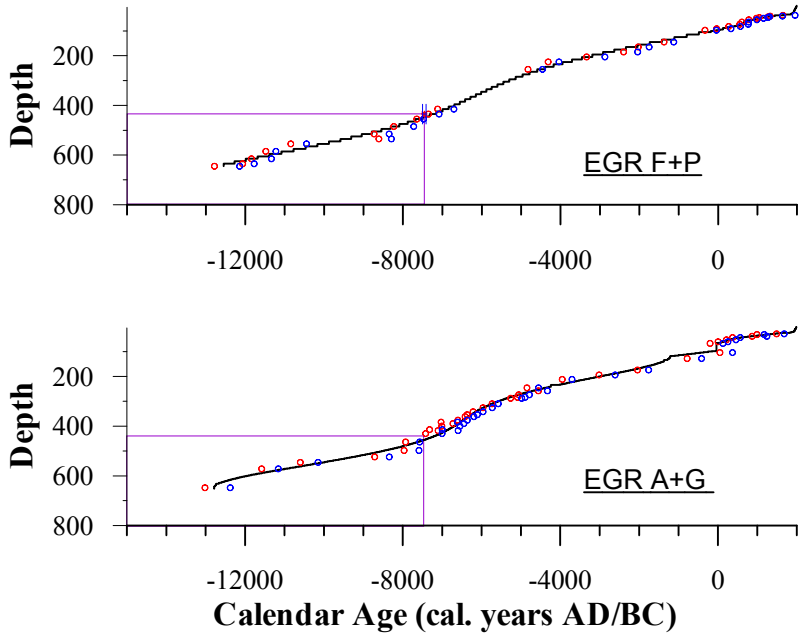

Figure DR 1. Age-depth models for the 2 cores EGR F+P and EGR A+G based on a 5 terms polynomial fit and IntCal04 terrestrial radiocarbon age calibration.. Black lines: age depth models; red circles: lower bound of the individual 95% confidence interval cal. ages given by OxCal. ; blue circles: upper bound of the individual 95% confidence interval cal. ages given by OxCal.

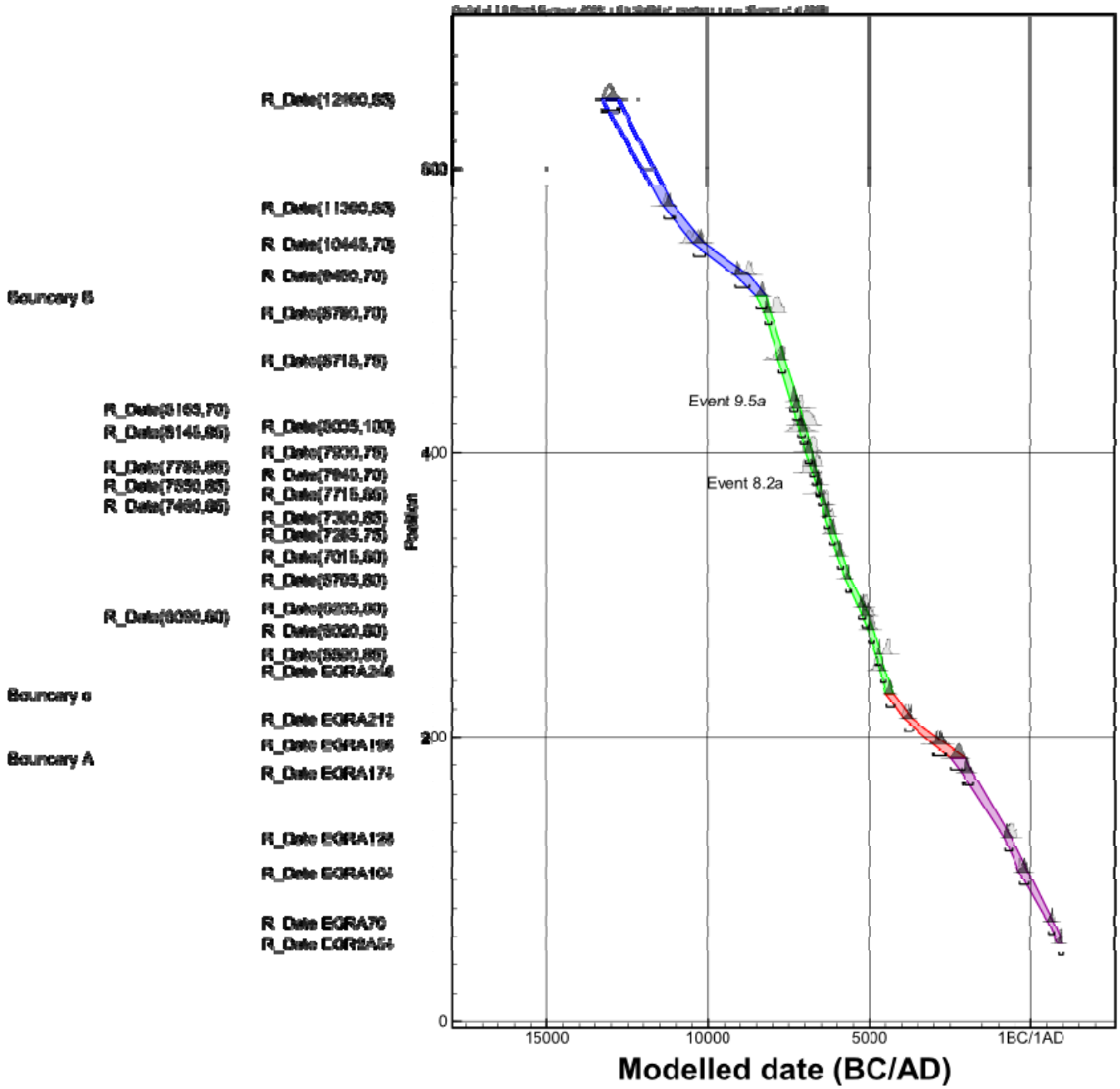

Figure DR 2. Oxcal v.4.1. age-depth model for EGR A+G.

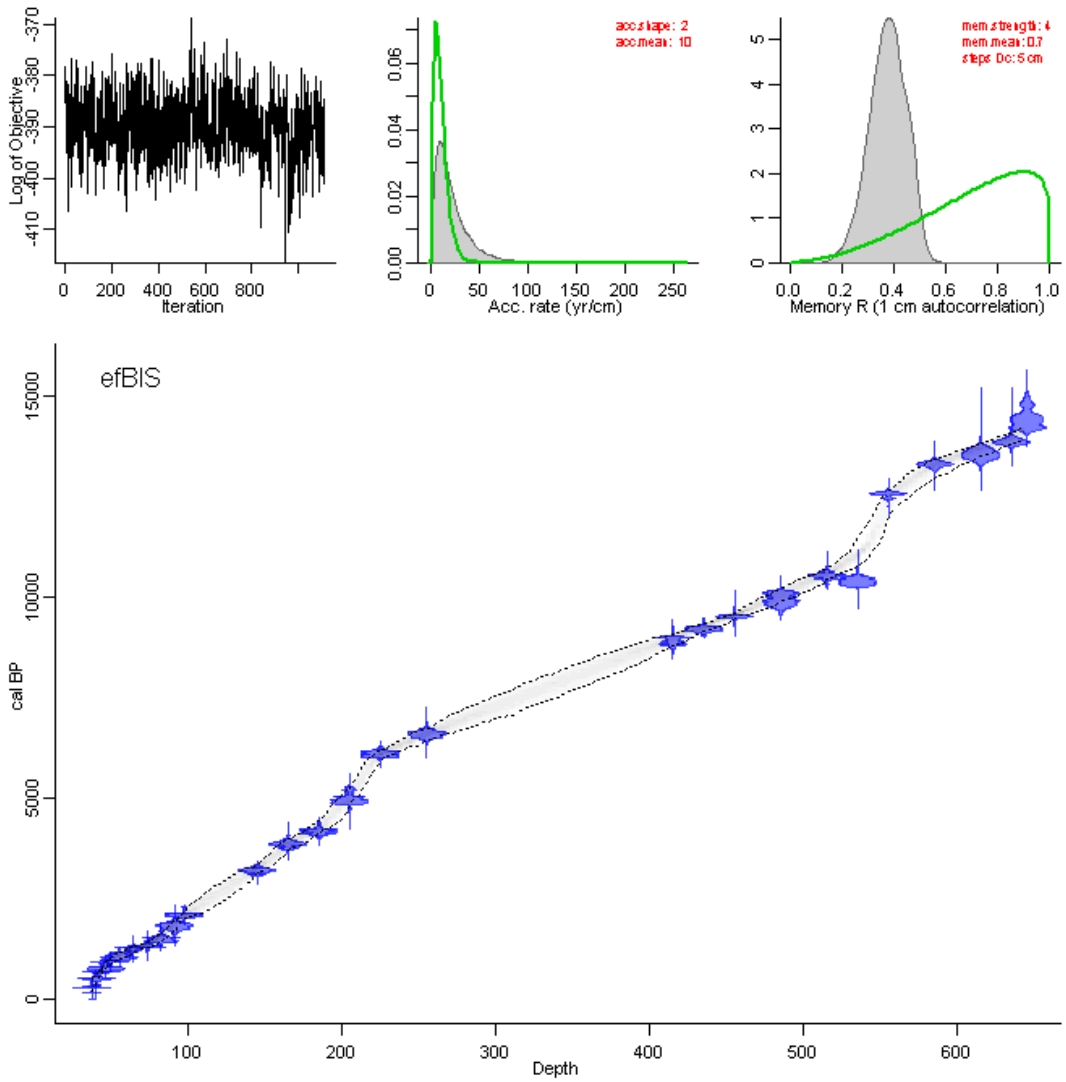

Figure DR 3. Age-depth model built with Bacon for EGR2E+2F (Blaauw and Christen, submitted). Darker colours indicate more likely calendar ages for the low-resolution core (depth in cm).

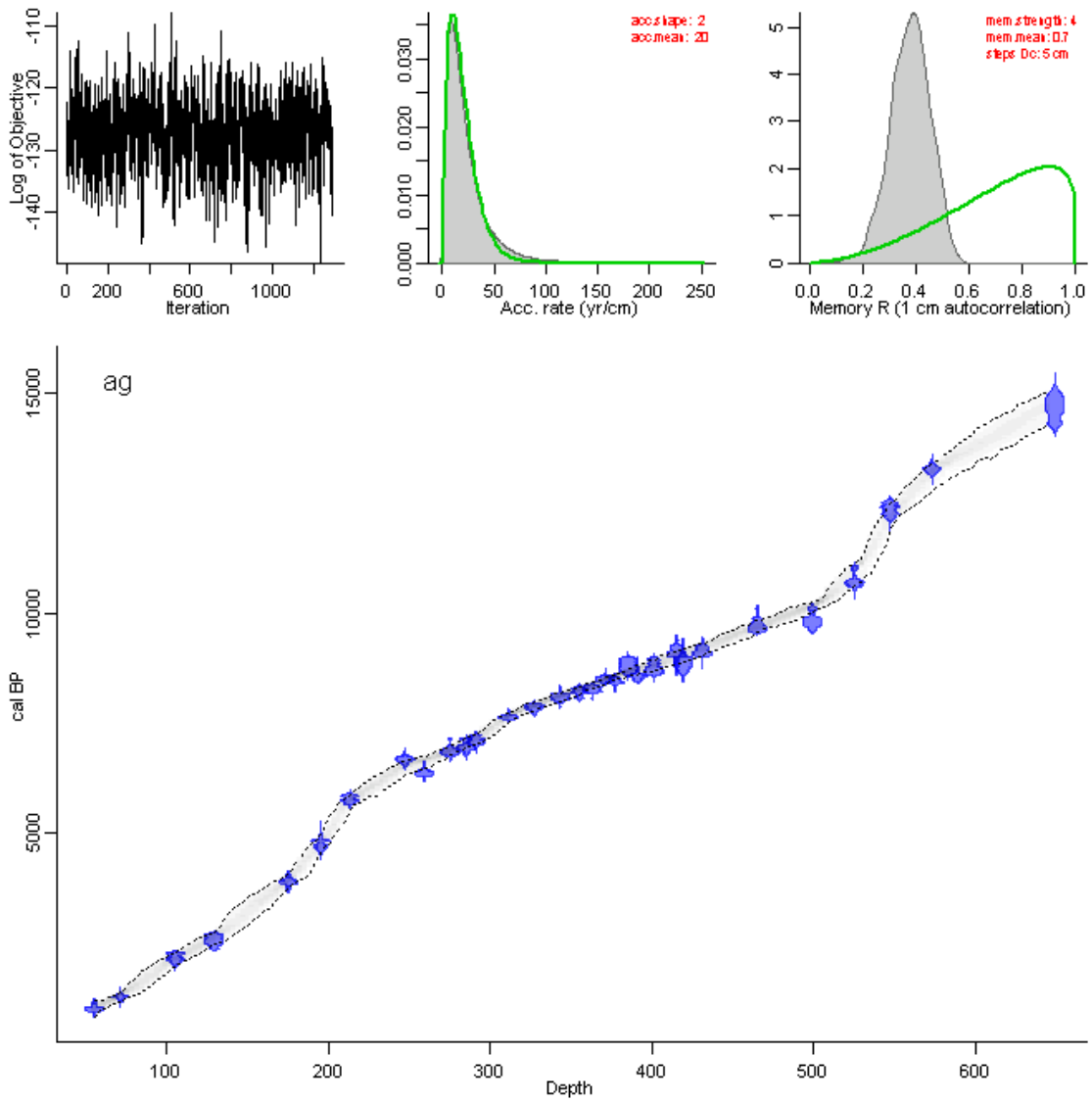

Figure DR 4. Age-depth model built with Bacon for core 2A+2G (Blaauw and Christen, submitted). Darker colours indicate more likely ages for the high-resolution core (depth in cm).

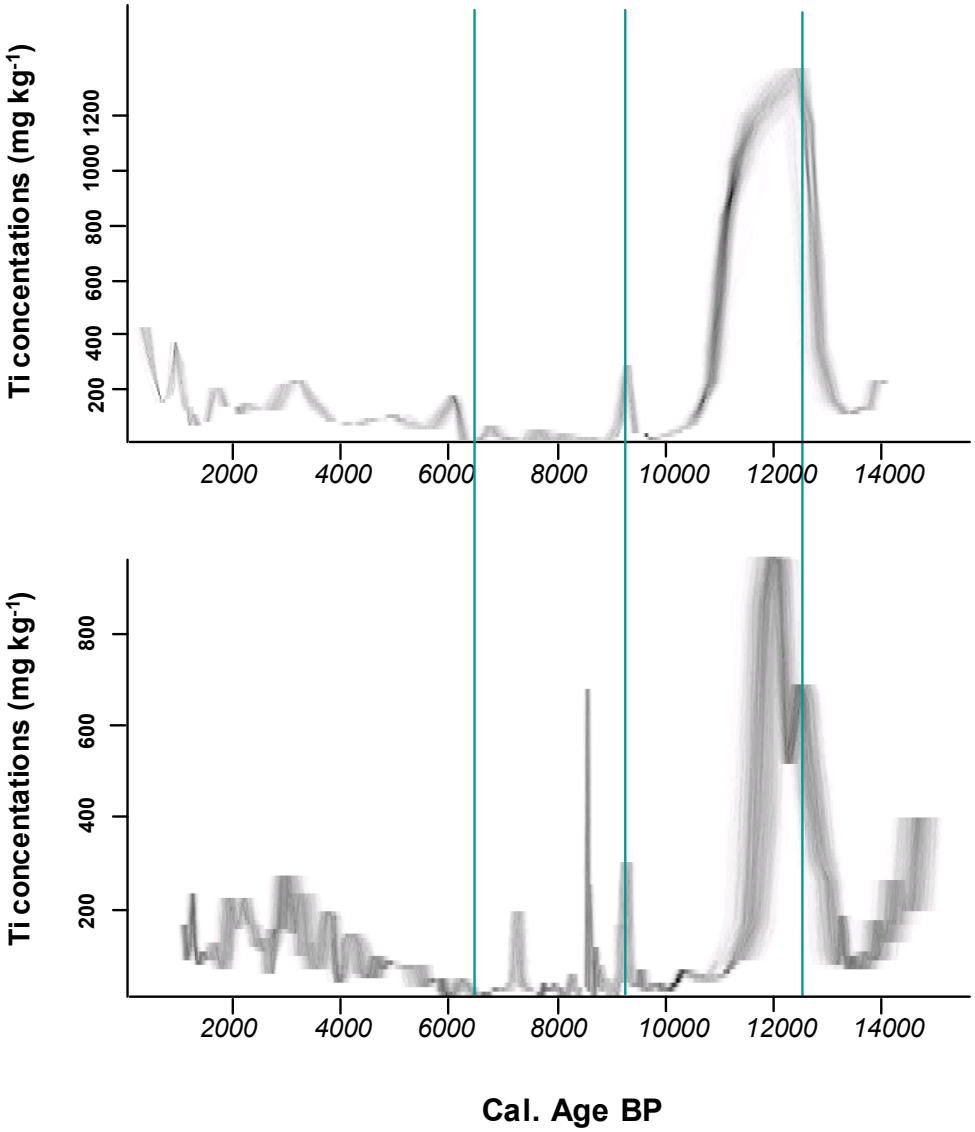

Figure DR 5. Ti concentration profiles in the low-(top) and high- (bottom) resolution core. Green lines are only visual outlines.

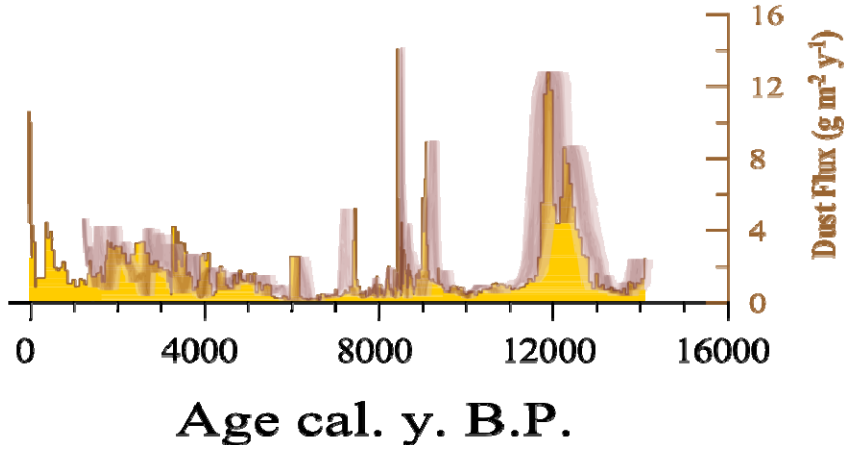

Figure DR6. Dust accumulation rate chronology in the high-resolution core based on the 5th polynomial model (yellow area) compared to the chronology built using Bacon for core 2A+2G (darker red colours indicate more likely ages).

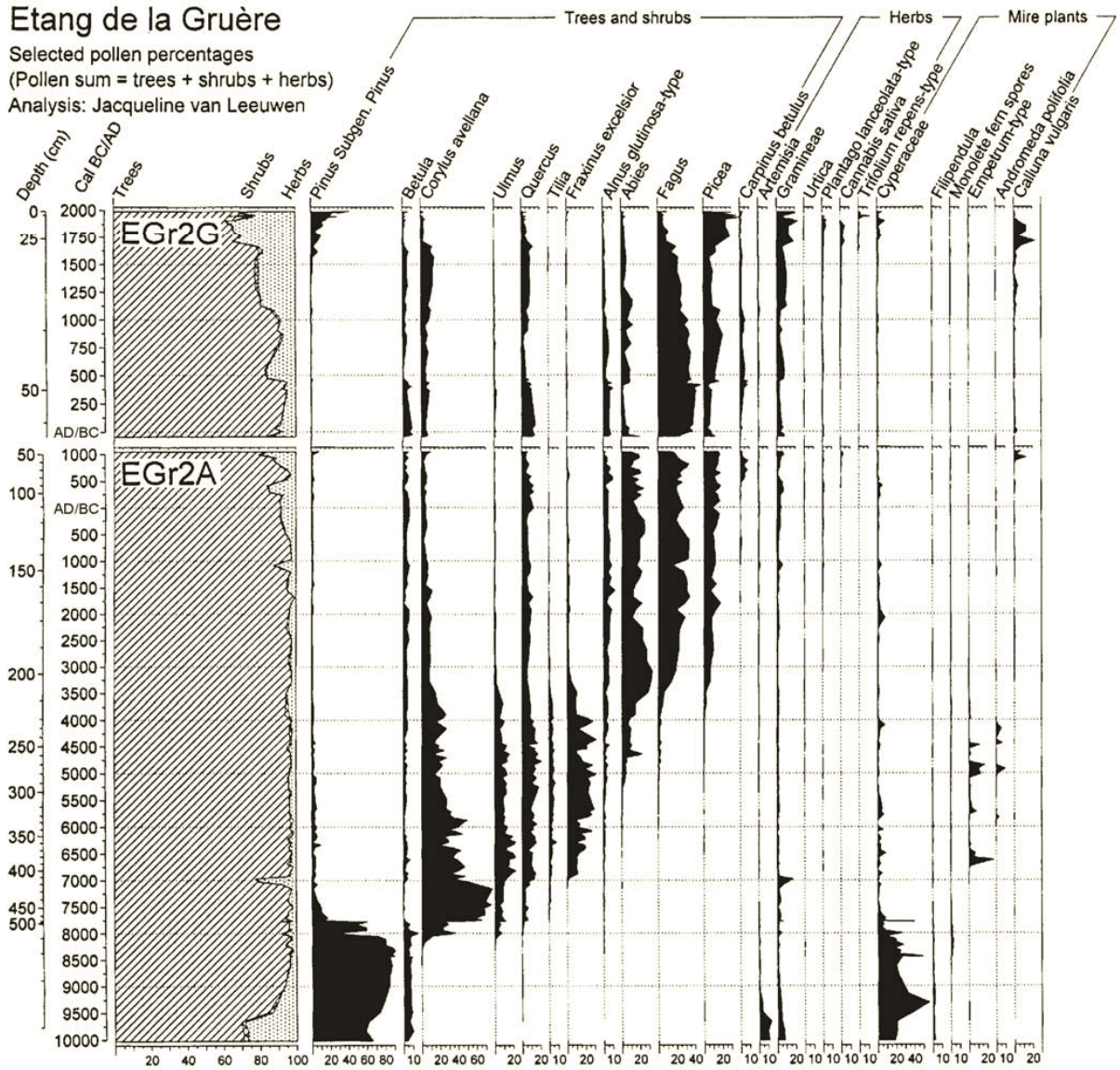

Figure DR7. Relative pollen abundances in the high-resolution core.